Front. Optoelectron. China 2010, 3(3): 317–320
DOI 10.1007/s12200-010-0104-y

RESEARCH ARTICLE

Tunable wettability of metallic films with assistance of porous anodic aluminum oxide

Dongdong LI[1,2], Chuanhai JIANG (✉)[2], Jiankun ZHOU[2,3], Xin REN[2]

1 Division of Energy and Environmental Research, Shanghai Advanced Research Institute, Chinese Academy of Sciences, Shanghai 201203, China
2 School of Material Science and Engineering, Shanghai Jiao Tong University, Shanghai 200240, China
3 Advanced Technology Institute, Technology Center of Baosteel, Shanghai 201900, China

Abstract The present work demonstrates a simple method to prepare nanostructured Ni films with different morphologies with the assistance of porous anodic aluminum oxide (AAO) membranes. A great distinction is observed as the Ni films deposited onto the top and bottom sides of AAO membranes. The wetting properties of as-prepared membranes are investigated by measuring the contact angles of water on the surfaces. Results show that the static water contact angle changes dramatically from 124°±1° to 45°±1° on different Ni films, implying a change of the wettability from hydrophobicity to hydrophilicity affected by the surface patterns. This versatile approach can be conducted on various materials with potential applications in a broad range of fields.

Keywords wettability, anodic aluminum oxide (AAO), Ni film

1 Introduction

Nanostructural materials are currently of great interest among researchers due to their promising applications in a large variety of fields [1–3]. Among the synthesis approaches, 'template method' has been proven to be a cheap and facile process in preparing zero-dimensional (0-D) and one-dimensional (1-D) arrays with the confinement of vertical aligned channels [3–11]. A commonly used template is the porous anodic aluminum oxide (AAO), which provides uniform nanoporous structures with controlled diameters and film thickness under specific conditions [12,13]. Inspired by the discovery of self-cleaning effect of Lotus leaves [14,15], extensive efforts have been devoted to developing superhydrophobic surfaces due to their potential applications in microfluidic devices, self-cleaning materials, water proof and anti-rain textiles, etc. [16–20]. By employing an AAO template, Pt nanowire arrays have been demonstrated with super-hydrophobic characteristic with the assistance of chemical modification [8].

Although AAOs have been widely used to synthesize various nanostructured materials, the hexagonal close-packed protuberances at the bottom used to be neglected and selectively removed in the template synthesis approach. Herein, we present a simple process to fabricate nanodot and nanoconcave membranes by employing both sides of AAO membranes. As a demonstration, Ni, which is widely used in mechanical, electroplating and rocketry industries, is utilized to construct the film. The morphology and microstructure of the obtained films are systematically characterized by scanning electron microscopy (SEM). The wetting properties of Ni patterns evaporated on the two sides of AAO surfaces as well as the smooth Ni film deposited on the Si substrate are characterized by a contact angle meter.

2 Experiments

AAO membranes are used as templates to fabricated Ni films with different morphologies. In brief, aluminum foils (0.3 mm thickness, 99.999% purity) are used as the starting material after annealing treatment at 450°C for 5 h, which are first anodized in 0.3 M oxalic acid at 60 V and 7°C for 4 h. And after etching the as-formed porous layer, the second-step anodization is carried out under identical conditions yielding the porous film with the pore diameter (D_p) of ~50 nm, interpore distance (D_{int}) of ~150 nm and film thickness of >60 μm [5–7]. The duration of the second-step anodization is typically more than 12 h, which ensures sufficient mechanical strength for the following process.

Received March 16, 2010; accepted March 28, 2010

E-mail: jiangchuanhai@gmail.com

Figure 1 illustrates the fabrication process of Ni membranes with different surface morphologies. The Ni nanodot arrays are formed in the AAO pores by electron-beam evaporation at a rate of 0.2 nm/s for a duration of 1000 s (Figs. 1(a) to 1(c)). Further deposition leads to a uniform film on top of AAO. The height of nanodots corresponding to the penetration length is determined by the pore diameter and the deposition rate. To realize the nanoconcave arrays, the AAO samples are submerged into saturated $HgCl_2$ or $SnCl_4$ aqueous solution to selectively remove the unwanted Al foils. The exposed barrier layer with round protuberances is now available for the following evaporation. Around 200 nm Ni membrane is deposited to duplicate the surface structure with the same condition as above. After the deposition, the metal surfaces are coated by epoxy for the following handling as described in Ref. [7]. Chemical etching is then carried out in 1 M NaOH solution to remove the unwanted AAO and aluminum. Metallic membranes with nanodot (Fig. 1(c)) and nanoconcave (Fig. 1(f)) arrays are available for the following measurements. For comparison, a 200-nm-thick Ni film is also deposited onto a Si (100) wafer forming a smooth membrane.

3 Results and discussion

Nickel or nickel-based alloy is a hydrophilic material, whose smooth surface has a water contact angle less than 90° as the following represented. However, the rough topography has been proved to be a prerequisite in tuning wetting properties [16]. Figure 2(a) displays a smooth Ni film prepared by evaporating nickel directly onto a clean silicon wafer for the purpose of comparing the roughness effect. Figures 2(b) and 2(c) show the SEM images of the nickel membranes deposited on the top and bottom sides of the AAO membranes, respectively. The surface morphologies of Ni films show great distinction between the evaporations on different sides of AAOs. Highly ordered Ni dot patterns with uniform dot size of ~50 nm can be observed in the enlarged image (inset of Fig. 2(b)), which is accordant with the pore diameter of AAO. The inset of Fig. 2(c) depicts the bottom morphology of as-obtained AAO. The electron-beam evaporation carried out on the bottom side of AAO leads to dense arrayed concave patterns as shown in Fig. 2(c). The inter-concave distance (~150 nm) is identical to the size of the interpore distance of AAO.

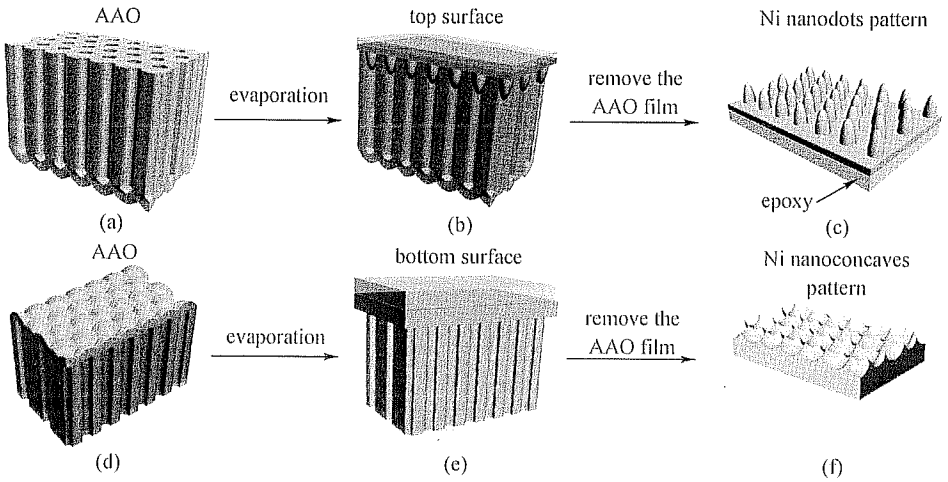

Fig. 1 Schematic diagram for preparation of Ni

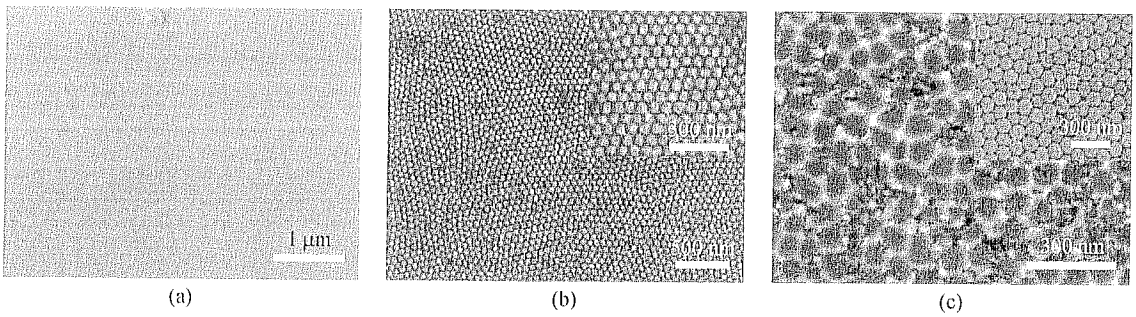

Fig. 2 SEM images of nickel membranes. (a) Deposited on a clean silicon wafer; (b) deposited on top surface of AAO (inset is a close-view image); (c) deposited on bottom surfaces of AAO (inset is a SEM image of AAO bottom before metal coating)

The wettabilities of these membranes are evaluated by static contact angle measurements. Figures 3(a) to 3(c) demonstrate the profiles of water droplets on the corresponding surfaces shown in Figs. 2(a) to 2(c). The smooth Ni film shows hydrophilicity with a static water contact angle of 82°±1°. Interestingly, the nanodot film yields an increased contact angle of 124°±1°, while the contact angle is significantly reduced to 45°±1° on the nanoconcave film. This implies that the surface patterns cause an opposite effect in the wettability, i.e., the nanodots lead to a hydrophobic behavior while nanoconcaves result in a more hydrophilic film.

The experimental results can be explained by Wenzel's law [21]:

$$\cos\theta_r = r\cos\theta, \tag{1}$$

which was first derived to describe the contact angle for a liquid droplet at a rough solid surface. In Eq. (1), θ_r and θ are the water contact angles on a rough surface and on a smooth surface made of the same material, respectively; r is the roughness factor. We can deduce from the above equation that the actual water contact angle decreases for hydrophilic materials ($\theta < 90°$) and increases for hydrophobic materials ($\theta > 90°$) with the increase of surface roughness. Owing to the hydrophilic property of Ni membrane ($\theta < 90°$) as shown in Fig. 3(a), it can be understood that the contact angle decreases to be about 45° for nanoconcave films (Fig. 3(c)).

Compared with these membranes deposited on the smooth silicon wafer and the bottom surface of AAO, the membrane obtained from the top AAO surface shows favorable hydrophobicity. The water contact angle in this case reaches as high as 124° as shown in Fig. 3(b). The morphology of highly ordered Ni nanodots is similar to the protrusions of the subtle surface features of Lotus leaf which provides the prerequisite roughness on the surface [16]. This kind of structure can trap a large amount of air which prevents the penetration of the water droplet into the surface, yielding a hydrophobic property upon the surfaces. The transformation of wettability from hydrophilicity to hydrophobicity as a result of the surface patterns can be explained in terms of the Cassie-Baxter equation [22], as

$$\cos\theta_r = f_1\cos\theta - f_2, \tag{2}$$

where f_1 and f_2 are the fractions of the liquid-solid interface area and the liquid-air interface area, where $f_1 + f_2 = 1$. It can be deduced from the above equation that an increase of f_2 would increase the actual contact angle of the Ni film (θ_r). In the case of Ni nanodot film, we adopt 82° and 124° as the water contact angle on the smooth (θ) and rough (θ_r) surfaces, respectively. Thus, f_2 is estimated to be 0.61, indicating that the formation of the nanodot pattern promotes large roughness. And a high proportion (~61%) of the air occupation in the contact area is responsible for the favorable hydrophobic property.

Similarly, Qu et al. [8] have reported such transformation from hydrophilicity to superhydrophobicity on the surface of Pt nanowire arrays. However, fluoroalkylsilane or other modification materials were used as hydrophobic coatings to impart the surface with low free energy in that case. The method of evaporation on the AAO template used in this study is more facile and cost-effective compared with other top-down approaches, such as deep silicon dry etching [23], anisotropic plasma etching [24] and X-ray lithography [25], which are usually employed in mimicking superhydrophobic biosurfaces. It is also reasonable to expect that the morphology of Ni pattern can be adjusted by regulating the geometries of AAO which could further tailor the water contact angle. Besides metallic films, the versatile process can be conducted on a variety of functional polymers, e.g., polydimethylsiloxane (PDMS), to construct flexible films with tunable wettability for practical applications.

4 Conclusions

In summary, nanostructured Ni films with different morphologies have been successfully prepared on AAO

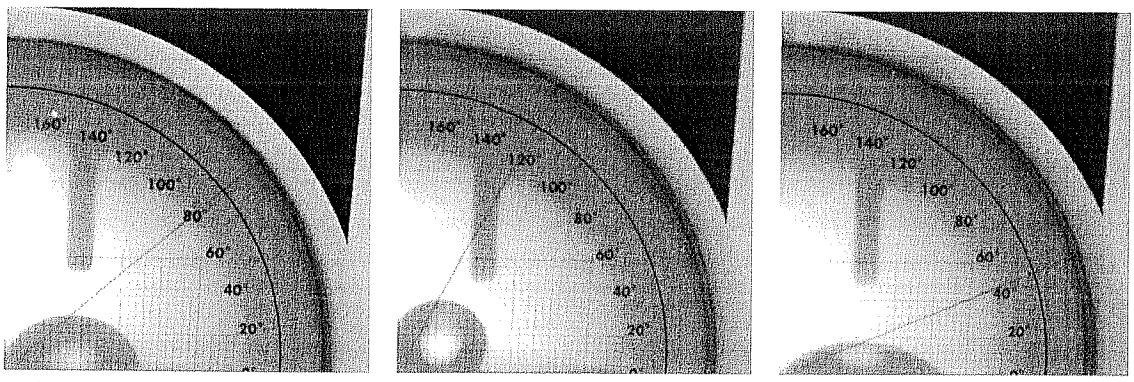

Fig. 3 Wettability of Ni films. (a) Smooth surface; (b) surfaces patterned with nanodot; (c) surfaces patterned with nanoconcave arrays

membranes by utilizing e-beam evaporation. The results show that the wettability of membranes strongly depends on the structure and subtle pattern of the film surface. The nanoconcaved Ni film shows a hydrophilic characteristic with the static water contact angle of 45°±1°. On the contrary, the contact angle reaches as high as 124°±1° on nanodot Ni film without any chemical modification, showing a favorable hydrophobicity. The Ni dot patterns provide a large roughness and a high proportion (~61%) of the air occupation in the droplet/film interface, which is responsible for the hydrophobic property.

Acknowledgements The work was supported by the International Scientific Collaboration Fund of Shanghai (No. 08520705300).

References

1. Ko H, Zhang Z X, Chueh Y L, Ho J C, Lee J, Fearing R S, Javey A. Wet and dry adhesion properties of self-selective nanowire connectors. Advanced Functional Materials, 2009, 19(19): 3098–3102
2. Lu J G, Chang P C, Fan Z Y. Quasi-one-dimensional metal oxide materials — synthesis, properties and applications. Materials Science and Engineering: R: Reports, 2006, 52(1–3): 49–91
3. Hurst S J, Payne E K, Qin L D, Mirkin C A. Multisegmented one-dimensional nanorods prepared by hard-template synthetic methods. Angewandte Chemie, 2006, 45(17): 2672–2692
4. Martin C R. Nanomaterials: a membrane-based synthetic approach. Science, 1994, 266(5193): 1961–1966
5. Li D, Jiang C, Jiang J, Lu J G. Self-assembly of periodic serrated nanostructures. Chemistry of Materials, 2009, 21(2): 253–258
6. Li D, Thompson R S, Bergmann G, Lu J G. Template-based synthesis and magnetic properties of cobalt nanotube arrays. Advanced Materials, 2008, 20(23): 4575–4578
7. Liu Z W, Chang P C, Chang C C, Galaktionov E, Bergmann G, Lu J G. Shape anisotropy and magnetization modulation in hexagonal cobalt nanowires. Advanced Functional Materials, 2008, 18(10): 1573–1578
8. Qu M, Zhao G Y, Wang Q, Cao X P, Zhang J. Fabrication of superhydrophobic surfaces by a Pt nanowire array on Ti/Si substrates. Nanotechnology, 2008, 19(19): 055707
9. Taberna P L, Mitra S, Poizot P, Simon P, Tarascon J-M. High rate capabilities Fe_3O_4-based Cu nano-architectured electrodes for lithium-ion battery applications. Nature Materials, 2006, 5(7): 567–573
10. Ding G Q, Shen W Z, Zheng M J, Xu W L, He Y L, Guo Q X. Fabrication of highly ordered nanocrystalline Si:H nanodots for the application of nanodevice arrays. Journal of Crystal Growth, 2005, 283(3–4): 339–345
11. Lei Y, Chim W K, Weissmuller J, Wilde G, Sun H P, Pan X Q. Ordered arrays of highly oriented single-crystal semiconductor nanoparticles on silicon substrates. Nanotechnology, 2005, 16(9): 1892–1898
12. Li A P, Müller F, Birner A, Nielsch K, Gösele U. Hexagonal pore arrays with a 50–420 nm interpore distance formed by self-organization in anodic alumina. Journal of Applied Physics, 1998, 84(11): 6023–6026
13. Lee W, Ji R, Gösele U, Nielsch K. Fast fabrication of long-range ordered porous alumina membranes by hard anodization. Nature Materials, 2006, 5(9): 741–747
14. Barthlott W, Neinhuis C. Purity of the sacred lotus, or escape from contamination in biological surfaces. Planta, 1997, 202(1): 1–8
15. Parkin I P, Palgrave R G. Self-cleaning coatings. Journal of Materials Chemistry, 2005, 15(17): 1689–1695
16. Zorba V, Stratakis E, Barberoglou M, Spanakis E, Tzanetakis P, Anastasiadis S H, Fotakis C. Biomimetic artificial surfaces quantitatively reproduce the water repellency of a lotus leaf. Advanced Materials, 2008, 20(21): 4049–4054
17. Blossey R. Self-cleaning surfaces — virtual realities. Nature Materials, 2003, 2(5): 301–306
18. Callies M, Quere D. On water repellency. Soft Matter, 2005, 1(1): 55–61
19. Nakajima A, Hashimoto K, Watanabe T. Recent studies on super-hydrophobic films. Monatshefte Fur Chemie, 2001, 132(1): 31–41
20. Hsu S H, Sigmund W M. Artificial hairy surfaces with a nearly perfect hydrophobic response. Langmuir, 2010, 26(3): 1504–1506
21. Wenzel R N. Resistance of solid surfaces to wetting by water. Industrial and Engineering Chemistry, 1936, 28: 988–994
22. Cassie A B D, Baxter S. Wettability of porous surfaces. Transactions of the Faraday Society, 1944, 40: 0546–0550
23. Krupenkin T N, Taylor J A, Schneider T M, Yang S. From rolling ball to complete wetting: the dynamic tuning of liquids on nanostructured surfaces. Langmuir, 2004, 20(10): 3824–3827
24. Dorrer C, Ruhe J. Wetting of silicon nanograss: from super-hydrophilic to superhydrophobic surfaces. Advanced Materials, 2008, 20(1): 159–163
25. Furstner R, Barthlott W, Neinhuis C, Walzel P. Wetting and self-cleaning properties of artificial superhydrophobic surfaces. Langmuir, 2005, 21(3): 956–961